Taylor & Francis
Taylor & Francis Group

BRIEF REPORT

8 OPEN ACCESS

Check for updates

Enhancing T cell anti-tumor efficacy with a PD1-TIGIT chimeric immune-checkpoint switch receptor

Jingjing Zhao[a]*, Jiebin Dong[a]*, Changwen Deng[b]*, Qianjing Zhang[a], Shicheng Sun[a], Honggang Li[a], Yun Bai[a], and Hongkui Deng[a,c]

[a]Department of Cell Biology and MOE Engineering Research Center of Regenerative Medicine, School of Basic Medical Sciences, State Key Laboratory of Natural and Biomimetic Drugs, Peking University Health Science Center, Peking University, Hadian District, Beijing, China; [b]Department of Respiratory and Critical Care Medicine, Shanghai East Hospital, School of medicine, Tongji University, Shanghai, China; [c]College of Life Sciences, Peking-Tsinghua Center for Life Sciences, Peking University, Beijing, China

ABSTRACT

Chimeric antigen receptor (CAR) T cell immunotherapy has demonstrated success in the treatment of hematological malignancies; however, its efficacy and applications in solid tumors remain limited. Immunosuppressive factors, particularly inhibitory checkpoint molecules, restrict CAR T cell activity inside solid tumors. The modulation of checkpoint pathways has emerged as a promising approach to promote anti-tumor responses in CAR T cells. Programmed cell death protein 1 (PD1) and T cell immunoreceptor with Ig and ITIM domains (TIGIT) are two critical immune-checkpoint molecules that suppress anti-tumor activity in T cells. Simultaneous targeting of these two inhibitory molecules could be an efficient checkpoint modulation strategy. Here, we developed a PD1-TIGIT chimeric immune-checkpoint switch receptor (CISR) that enhances the efficacy of CAR T cell immunotherapy by reversing the inhibitory checkpoint signals of PD1/PDL1 and/or TIGIT/CD155. In addition to neutralizing PDL1 and CD155, this chimeric receptor is engineered with the transmembrane region and intracellular domain of CD28, thereby effectively enhancing T cell survival and tumor-targeting functions. Notably, under simultaneous stimulation of PDL1 and CD155, CISR-CAR T cells demonstrate superior performance in terms of cell survival, proliferation, cytokine release, and cytotoxicity *in vitro*, compared with conventional CAR T cells. Experiments utilizing both cell line- and patient-derived xenotransplantation tumor models showed that CISR-CAR T cells exhibit robust infiltration and anti-tumor efficiency *in vivo*. Our results highlight the potential for the CISR strategy to enhance T cell anti-tumor efficacy and provide an alternative approach for T cell-based immunotherapies.

Introduction

Chimeric antigen receptor (CAR) T cell immunotherapy has been successful in the management of hematologic malignancies,[1] but its applications in solid tumors have been limited. Inhibitory immune checkpoints, particularly in the tumor microenvironment, contribute to this problem.[2] Checkpoint receptors such as programmed cell death protein 1 (PD1) and T cell immunoreceptor with Ig and ITIM domains (TIGIT) hinder T cell activity via ligand-based suppression of anti-tumor effects.[3,4] PD1 upregulation in activated T cells leads to exhaustion upon binding to its ligand PDL1, which is widely expressed by tumor cells in various cancers.[5] Similarly, TIGIT interacts with CD155, which is overexpressed in tumors and tumor-infiltrating myeloid cells; this interaction inhibits T cell responses.[6] The co-expression of PD1 and TIGIT on intratumoral T cells is associated with poor clinical outcomes and accelerated tumor progression.[7,8] Immune-checkpoint targeting via checkpoint inhibitors or genetic modifications of CAR T cells with PD1- or TIGIT-based receptors has

demonstrated potential in the promotion of anti-tumor responses.[9–12] However, considering the complex and diverse mechanisms underlying the effects of inhibitory molecules, targeting efforts focused on a single checkpoint pathway may be insufficient to achieve optimal T cell anti-tumor responses. Dual immune checkpoint blockade enhances T cell activity and outcomes in solid tumor treatment.[13–15]

The complexity of immunosuppressive molecules represents a major challenge for engineered T cell-based immunotherapies. To address this problem, a chimeric immune-checkpoint switch receptor (CISR) strategy is proposed, which utilizes a chimeric ectodomain that can bind two different immune checkpoint ligands, in combination with an engineered intracellular domain (ICD) that interacts with T cell survival and activation pathways. The PD1-TIGIT CISR recognizes PDL1 and CD155, converting negative signals into positive signals, thereby enhancing T cell anti-tumor activity. Experimental evidence has demonstrated the

superior performance of CISR-engineered CAR T cells in the treatment of solid tumors, both *in vitro* and in xenograft models.

Methods

Cell lines and culture conditions

Daudi, HCT116, and A549 cell lines were acquired from the National Infrastructure of Cell Line Resource (Beijing, China); HEK-293T cells were obtained from the American Type Culture Collection (USA). Daudi cells were cultured in RPMI 1640 medium (Gibco) with 10% fetal bovine serum (GEMINI), whereas HCT116, A549, and HEK-293T cells were cultured in Dulbecco's modified Eagle medium (Gibco) with 10% fetal bovine serum. All cells were cultured at 37°C with 5% CO_2.

Plasmid construction and lentivirus production

The DNA sequences of anti-epidermal growth factor receptor (EGFR) CARs (EGFRz-CAR and EGFRBBz-CAR) were synthesized by BGI Genomics (Beijing, China) and subcloned into the pRRLSIN.cPPT lentiviral vector. The CISR was constructed in a similar manner. PD1 extracellular domain (ECD), TIGIT ECD, and CD28 transmembrane region and ICD were fused by polymerase chain reaction. Each CAR was linked to the CISR using a P2A sequence and cloned into the pRRLSIN.cPPT vector to generate Ez.CISR and EBBz.CISR. Lentiviral supernatants were prepared as previously described.[16]

T cell culture and lentivirus transduction

All Peripheral Blood Mononuclear Cells (PBMCs) used in our study were obtained from healthy donors who provided informed consent (Blood Center of Beijing Red Cross Society). CD3+ T cells were isolated from PBMCs using a Human T Cell Enrichment Kit (STEMCELL Technologies). T cells were cultured in X-VIVO™ 15 medium (Lonza) with 10% fetal bovine serum and 100 U/mL interleukin (IL)-2 (PeproTech). T cell stimulation was performed with CD3/CD28 DynaBeads® (Thermo Fisher Scientific) at a bead-to-cell ratio of 1:1 for 48 hours; this step was followed by lentiviral transduction. IL-2-containing medium was refreshed every 2–3 days, and DynaBeads® were removed after 5 days.

Flow cytometry

Cells were stained with specific antibodies for flow cytometry analysis were used: anti-CD3 (BioLegend or BD Pharmingen), anti-CD4 (BD Pharmingen), anti-CD8 (BD Pharmingen), anti-EGFR (BioLegend), anti-PD1 (BioLegend), anti-TIGIT (BioLegend), anti-CD62L (BioLegend), anti-CD45RA (eBioscience), anti-CD155 (BioLegend), and anti-CD274 (PDL1; BioLegend). CAR expression was detected using an Alexa Fluor 647 antibody (Jackson ImmunoResearch). Flow cytometry was performed using a Beckman Coulter Flow Cytometer (Beckman Coulter, USA), and data were analyzed with CytExpert software.

Cytotoxicity assay

Tumor cell lines transduced to express EGFR, PDL1, and CD155 were sorted via flow cytometry to create target cells. CAR expression levels in different gene-modified T cells were equalized before cytotoxicity experiments. Short-term cytotoxicity (24 hours) was assessed using green fluorescent protein-firefly luciferase-transduced target cells at various effector-to-target ratios (0.3:1, 1:1, 3:1, and 9:1), then evaluated using a standard bioluminescence assay.[17] Long-term cytotoxicity (3 or 6 days) involved coculturing T cells and targets at effector-to-target (E:T) ratios of 1:15 or 1:25 on six-well plates, followed by fluorescence-activated cell sorting analysis to distinguish T cells and tumor cells according to CD3 expression.

Cytokine release assay

T cells and tumor cells were cocultured at E:T ratios of 1:1, 5:1, and 10:1 in 96-well plates. Human PDL1 (MedChemExpress) or human CD155 (MedChemExpress) at indicated concentrations were added when testing the impact of soluble forms of PDL1/CD155 on CISR. After 24 hours, supernatant was collected and cytokine release (IL-2, interferon [IFN]-γ, and tumor necrosis factor [TNF]-α) was measured using enzyme-linked immunosorbent assay kits (Dakewe Biotech), in accordance with the manufacturer's instructions.

In vitro coculture assay

A549-P tumor cells expressing EGFR, PDL1, and CD155 were seeded on 6-well plates (3×10^5 cells/well). Then, 1×10^6 EGFRBBz-CAR or EBBz.CISR T cells (both approximately 30% CAR-positive) were added to each well. T cells were collected and transferred every 2 days to a new plate with feeder cells; no additional cytokines were added during the experiment. The experiment durations were 8 days for T cell proliferation assays and 7 days for phenotype and cytotoxicity assays.

Animal experiments

Female NPG (NOD.Cg-Prkdc^scid Il2rg^tm1Vst/Vst) mice (6–8 weeks old) were purchased from Beijing Vitalstar Biotechnology. Colorectal carcinoma cell-derived xenograft models were established by subcutaneous injection of HCT116-P cells into NPG mice. CAR T cell treatment was administered intravenously when tumors reached specific volumes. Patient-derived xenograft (PDX) models were established using fresh tumor tissues derived from patients with colorectal cancer as described in our previous studies,[16] and T cells were administered intravenously when each tumor reached a specific volume. Tumor volume was measured every 3 days and calculated using the following formula: volume (mm^3) = (length × width × width)/2. Peripheral blood was analyzed by flow cytometry and cytokine release assays. Mice with large tumor masses were euthanized early because of ethical considerations. These protocols were approved by the Ethical Committee of Peking University Health Science Center

and the Institutional Animal Care and Use Committee of Beijing Vitalstar Biotechnology.

Histological and immunohistochemical analysis

Tumor tissues were fixed with 4% (w/v) paraformaldehyde solution, dehydrated in ethanol, embedded in paraffin, and cut into 3-μm serial sections for histological staining. Hematoxylin and eosin (Leica) staining was performed in a conventional manner. For immunohistochemical staining, primary antibodies against EGFR (Abcam), PDL1 (Abcam), CD155 (Cell Signaling Technology), and CD3 (Abcam) were used; the secondary antibody was horseradish peroxidase-conjugated goat anti-rabbit IgG (H+L) (Servicebio). Whole-slide images were collected using Panoramic DESK (3D HISTECH) and analyzed with Caseviewer C.V 2.3.

Statistical analysis

Statistical analyses were performed using Prism software version 8.0 (GraphPad). P-values were calculated using the tests specified in figure legends. Error bars represent standard deviations (SDs) or standard errors of the mean (SEMs) (specified in legends). Significance levels are indicated as follows: $*P < .05$, $**P < .01$, $***P < .001$, and $****P < .0001$. $P < .05$ was considered statistically significant.

Results

Design and functional validation of PD1-TIGIT CISR

PD1 and TIGIT are both common and critical immune checkpoint receptors that are upregulated on tumor-infiltrating T cells; their respective ligands, PDL1 and CD155, are overexpressed by tumor cells to suppress T cell activity.[7,18,19] To simultaneously target both signals, we designed a PD1-TIGIT CISR that combines the ECDs of PD1 and TIGIT with the transmembrane region and ICD of CD28, an important T cell co-stimulatory molecule[20,21] (Figure 1a). We hypothesized that this chimeric receptor would activate the intracellular co-stimulatory CD28 signaling pathway upon binding to PDL1 or CD155, thereby reversing inhibitory PD1/TIGIT signals in anti-tumor T cells.

To validate CISR function, we used a P2A sequence to link the CISR with an anti-EGFR CAR, creating Ez.CISR (Figure 1b). Flow cytometry analysis of CD3$^+$ T cells that had been transduced with EGFRz-CAR or Ez.CISR revealed the expression of PD1 and TIGIT in a portion of activated T cells and EGFRz-CAR T cells, with high co-expression of PD1/TIGIT and CAR molecules in Ez.CISR-transduced T cells; these results indicated successful transduction and expression of the CISR (Figure S1). Next, we investigated whether the CISR could interact with PDL1 or CD155 and activate the engineered intracellular CD28 signal. For separate stimulation of the PD1 and TIGIT domains of the CISR, Daudi cells were genetically modified to express EGFR, PDL1, and CD155, generating EGFR-expressing Daudi cells (Daudi-E), PDL1-expressing Daudi-E cells (Daudi-E.P), and CD155-expressing Daudi-E cells (Daudi-E.155) (Figure S2). CISR activation was expected to enhance cytokine release by

Ez.CISR T cells because of the functional characteristics of CD28. Stimulation with PDL1 or CD155 significantly increased cytokine release (IL-2, IFN-γ, and TNF-α) by Ez. CISR T cells, indicating activation of CD28 signaling. In contrast, the presence of PDL1 or CD155 did not enhance (and sometimes reduced) cytokine release from EGFRz-CAR T cells (Figures 1c,d and S3a-d).

After confirming the feasibility of the CISR, we investigated its ability to enhance activity in second-generation CAR T cells, which have demonstrated increased efficacy in preclinical studies and clinical trials but are limited by the immunosuppressive microenvironment in solid tumors. We examined the functionality of CISR in combination with an anti-EGFR CAR containing a 4-1BB co-stimulatory molecule (EGFRBBz-CAR), which constituted EBBz.CISR (Figure 1e). Successful expression of the CISR was observed in CAR-positive EBBz. CISR T cells (Figure S4). In ex vivo cultures, EBBz.CISR T cells exhibited a more rapid increase in the proportion of CD8$^+$ cells, compared with EGFRBBz-CAR T cells (Figure S5). Although the presence of 4-1BB in EGFRBBz-CAR can improve effector cytokine release,[22] further activation of EBBz.CISR T cells was achieved via stimulation with PDL1 or CD155 (Figures 1f,g and S6a-d). Besides, we cocultured EBBz. CISR T cells with Daudi-E cells at the presence of soluble forms of PDL1 (sPDL1) or CD155 (sCD155). However, no increase in cytokine release was detected by the presence of either sPDL1 or sCD155 (Figure S7a, b), suggesting that CISR could not be activated by the soluble forms of PDL1 and CD155. In summary, these findings demonstrate the functional conversion of inhibitory immune checkpoint signals by the CISR through the activation of a co-stimulatory pathway upon recognition of PDL1 or CD155 expressed on tumor cells.

EBBz.CISR T cells maintained superior performance in ex vivo dual suppressive environments

The anti-tumor effects of EBBz.CISR T cells were assessed using tumor cells expressing both PDL1 and CD155. HCT116 (human colorectal carcinoma cell line) and A549 (human non-small-cell lung carcinoma cell line) naturally express high levels of EGFR and CD155 (Figure S8a, b). Accordingly, we generated two new cell lines, HCT116-P and A549-P, which overexpressed PDL1; these cell lines mimicked a dual suppressive tumor environment (Figure S8c). Cytokine release from T cells was evaluated after coculture with HCT116-P or A549-P cells; levels of IL-2 and IFN-γ released from EBBz.CISR T cells were higher than the levels released from EGFRBBz-CAR T cells (Figures 1h and S9a). Cytotoxicity assays using HCT116-P cells revealed a superior anti-tumor effect in the EBBz.CISR group, compared with the EGFRBBz-CAR group, such that fewer tumor cells remained after 3 days of coculture involving CAR T cells and tumor cells at an E:T ratio of 1:15 (Figure S9b). When the E:T ratio was reduced to 1:25, the EBBz.CISR group also displayed significantly improved cytolytic efficacy against tumor cells on days 3 and 6, compared with the EGFRBBz-CAR group (Figure S9c). Thus, EBBz.CISR demonstrated enhanced cytokine release and cytolytic efficacy against tumor cells in a dual suppressive environment.
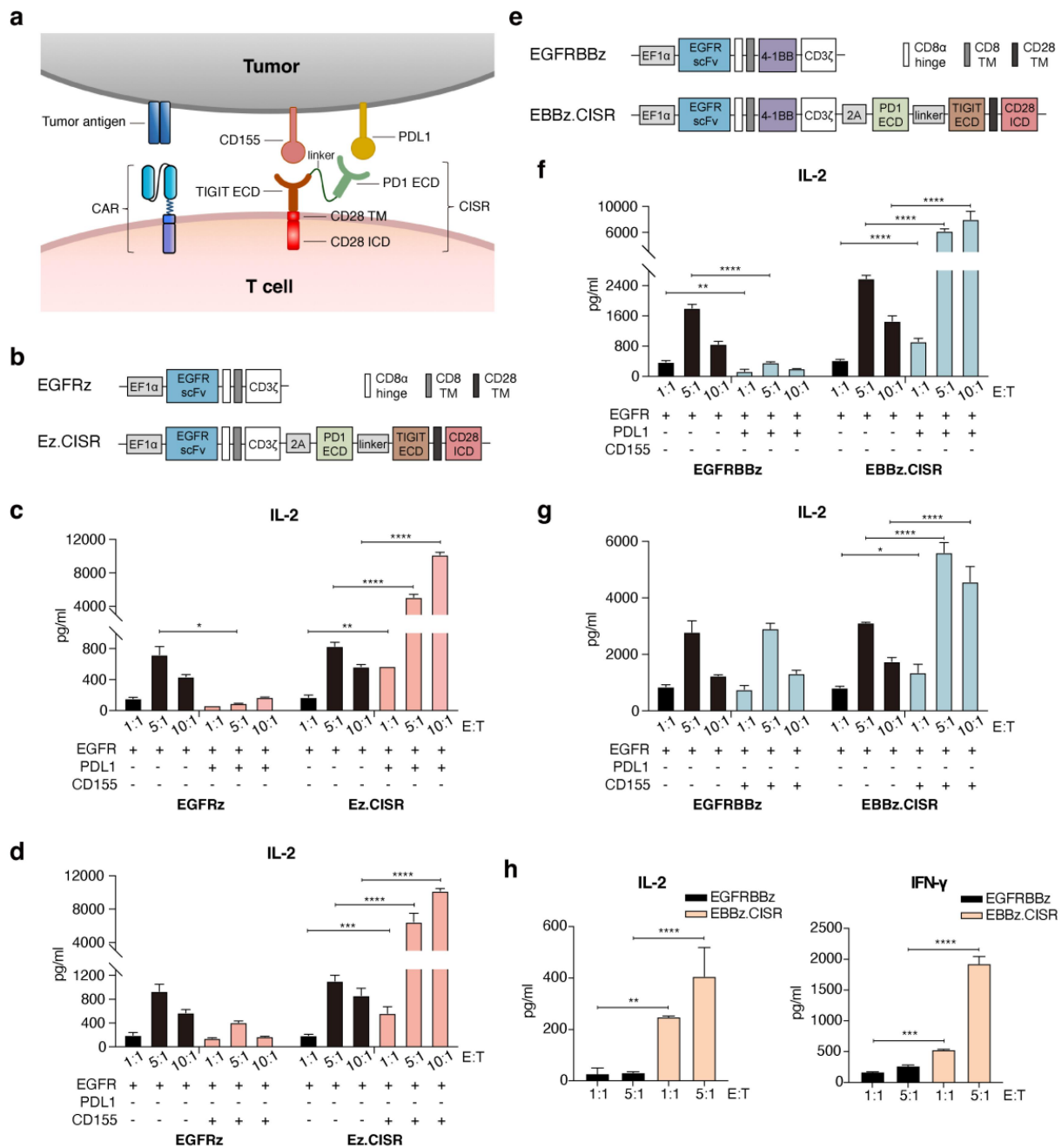
Figure 1. Design, signal activation, and functional validation of the PD1-TIGIT CISR. (a) schematic representation of the CISR. The extracellular domain (ECD) of the CISR consists of the TIGIT ECD and the PD1 ECD, connected by a linker. The newly designed extracellular recognition region is fused to the transmembrane (TM) region and intracellular domain (ICD) of CD28. The CISR binds to PDL1 and CD155 molecules on tumor cells, delivering a positive signal to activate intracellular CD28 signaling. (b) schematic representation of the anti-EGFR CAR (EGFRz-CAR) and the EGFRz-CAR linked to the CISR (Ez.CISR). (c, d) coculture of EGFRz-CAR T cells or Ez.CISR T cells with target cells (c, Daudi-E and Daudi-E.P cells; d, Daudi-E cells and Daudi-E.155 cells) at E:T ratios of 1:1, 5:1, and 10:1. After 24 hours, culture supernatants were collected, and levels of IL-2 were measured by enzyme-linked immunosorbent assays (means ± SDs, $n = 3$). Statistical significance in panels (c) and (d) was analyzed using two-way analysis of variance (ANOVA); *$P < .1$, **$P < .01$, ***$P < .001$, ****$P < .0001$. (e) schematic representation of the anti-EGFR CAR with the 4-1BB co-stimulatory molecule (EGFRBBz-CAR) and the EGFRBBz-CAR linked to the CISR (EBBz.CISR). (f, g) coculture of EGFRBBz-CAR T cells or EBBz.CISR T cells with target cells (f, Daudi-E and Daudi-E.P cells; g, Daudi-E cells and Daudi-E.155 cells) at E:T ratios of 1:1, 5:1, and 10:1. Culture supernatants were collected after 24 hours to measure levels of IL-2 (means ± SDs, $n = 3$). Data were analyzed using two-way ANOVA; *$P < .1$, **$P < .01$, ****$P < .0001$. (h) coculture of T cells with EGFR⁺PDL1⁺CD155⁺ HCT116-P cells at E:T ratios of 1:1 and 5:1. After 24 hours, culture supernatants were collected, and levels of IL-2 and IFN-γ were measured (means ± SDs, $n = 3$). Data were analyzed using two-way ANOVA; **$P < .01$, ***$P < .001$, ****$P < .0001$.

To assess the functional advantages of EBBz.CISR T cells in an immunosuppressive tumor microenvironment, we developed a coculture system using A549-P cells to model a tumor environment consisting of continuous stimulation via EGFR, PDL1, and CD155 (Figure 2a). Interactions of PD1 and TIGIT with their ligands transmit intracellular signals that inhibit T cell proliferation.[6,23] During 1 week of exposure to this tumor environment, EGFRBBz-CAR T cell numbers initially increased, then gradually decreased (Figure 2b). In contrast, EBBz.CISR T cells exhibited improved proliferation activity, with a nearly 20-fold increase in cell number from day 0 to day 8 (Figure 2b). CISR activation successfully reversed the inhibition of proliferation that was induced by inhibitory immune checkpoint signals.
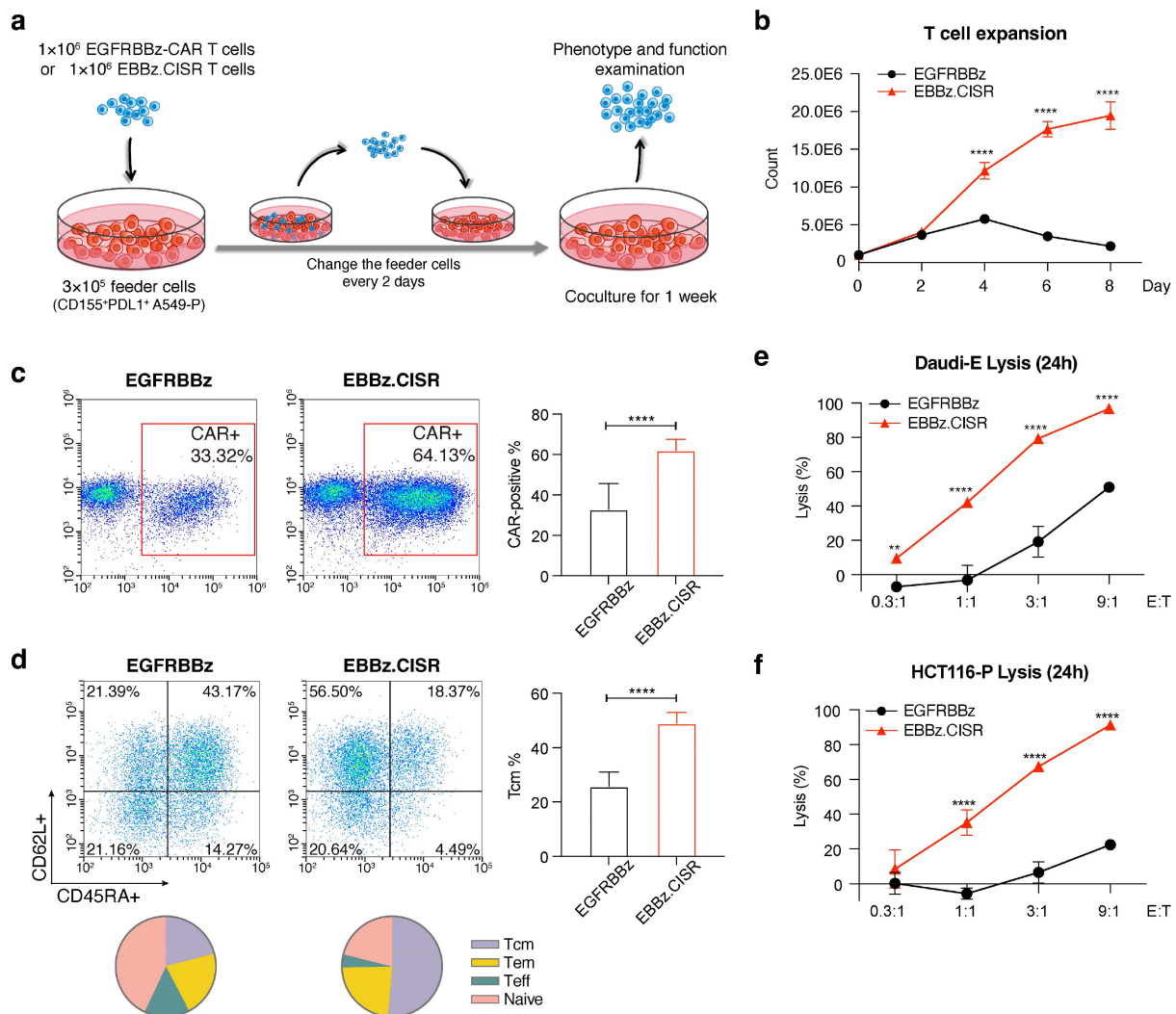
Figure 2. Performance of EBBz.CISR after prolonged exposure to a suppressive tumor environment. (a) schematic representation of the coculture system. EGFR⁺PDL1⁺CD155⁺ A549-P tumor cells were seeded overnight in 6-well plates (3×10^5 cells/well) to generate feeder cells. On Day 0, 1×10^6 EGFRBBz-CAR T cells or EBBz.CISR T cells (both approximately 30% CAR-positive) were added. Every 2 days, the cocultured T cells were separated, counted, and transferred into a new plate with fresh feeder cells. T cells were cocultured for 8 days or collected on day 7 for phenotype and cytotoxicity analyses. (b) cell counts of T cells cocultured with A549-P cells (means ± SDs, $n = 3$). Data were analyzed using two-way ANOVA; *$P < .0001$. (c) CAR expression in cocultured T cells was detected by flow cytometry. Representative donor is shown (left panel), along with summary data (right panel; means ± SDs, $n = 9$) of nine independent experiments with T cells from three different donors. Data were analyzed using two-tailed Student's t-test; **$P < .0001$. (d) memory phenotypes of cocultured T cells were detected by flow cytometry using anti-CD62L and anti-CD45RA antibodies. Central memory T cell (Tcm, CD62L⁺CD45RA⁻), effector memory T cell (tem, CD62L⁻CD45RA⁻), effector T cell (teff, CD62L⁻CD45RA⁺), and naïve T cell (CD62L⁺CD45RA⁺) phenotypes were present. Representative donor is shown (left panel), along with summary data (right panel; means ± SDs, $n = 6$) of six independent experiments with T cells from two different donors. Data were analyzed using two-tailed Student's t-test; ***$P < .0001$. (e, f) cytotoxicity of cocultured T cells was measured through a second coculture experiment using EGFR⁺PDL1⁻CD155⁻ Daudi-E cells or EGFR⁺PDL1⁺CD155⁺ HCT116-P cells at indicated E:T ratios for 24 hours (means ± SDs, $n = 3$). Data were analyzed using two-way ANOVA; ****$P < .01$, *$P < .0001$.

Next, we examined CAR expression and memory phenotype in T cells that had been subjected to coculture experiments. EBBz.CISR T cells showed greater enrichment of CAR-positive cells, compared with EGFRBBz-CAR T cells (Figure 2c). Additionally, the proportion of central memory T cells (Tcm), which could display better persistence and anti-tumor immunity,[24] was higher in EBBz.CISR T cells than in EGFRBBz-CAR T cells (Figure 2d). These findings indicate that EBBz.CISR T cells maintain favorable characteristics under suppressive conditions. We also tested cytolytic activity of T cells generated in coculture experiments. EBBz.CISR T cells exhibited significantly higher tumor lysis activity, compared with EGFRBBz-CAR T cells, when targeting Daudi-E cells or HCT116-P cells (Figure 2e,f). Overall, under tumor-mimicking conditions, EBBz.CISR T cells demonstrated enhanced function in terms of cell proliferation, CAR-positive enrichment, memory phenotype, and cytotoxicity maintenance; all of these factors contribute to improvements in T cell anti-tumor activity.

CISR enhances T cell anti-tumor efficacy in vivo

Colorectal cancers are some of the most common and lethal cancers worldwide.[25] PD1 and TIGIT, both upregulated in colorectal cancers, are associated with T cell dysfunction and
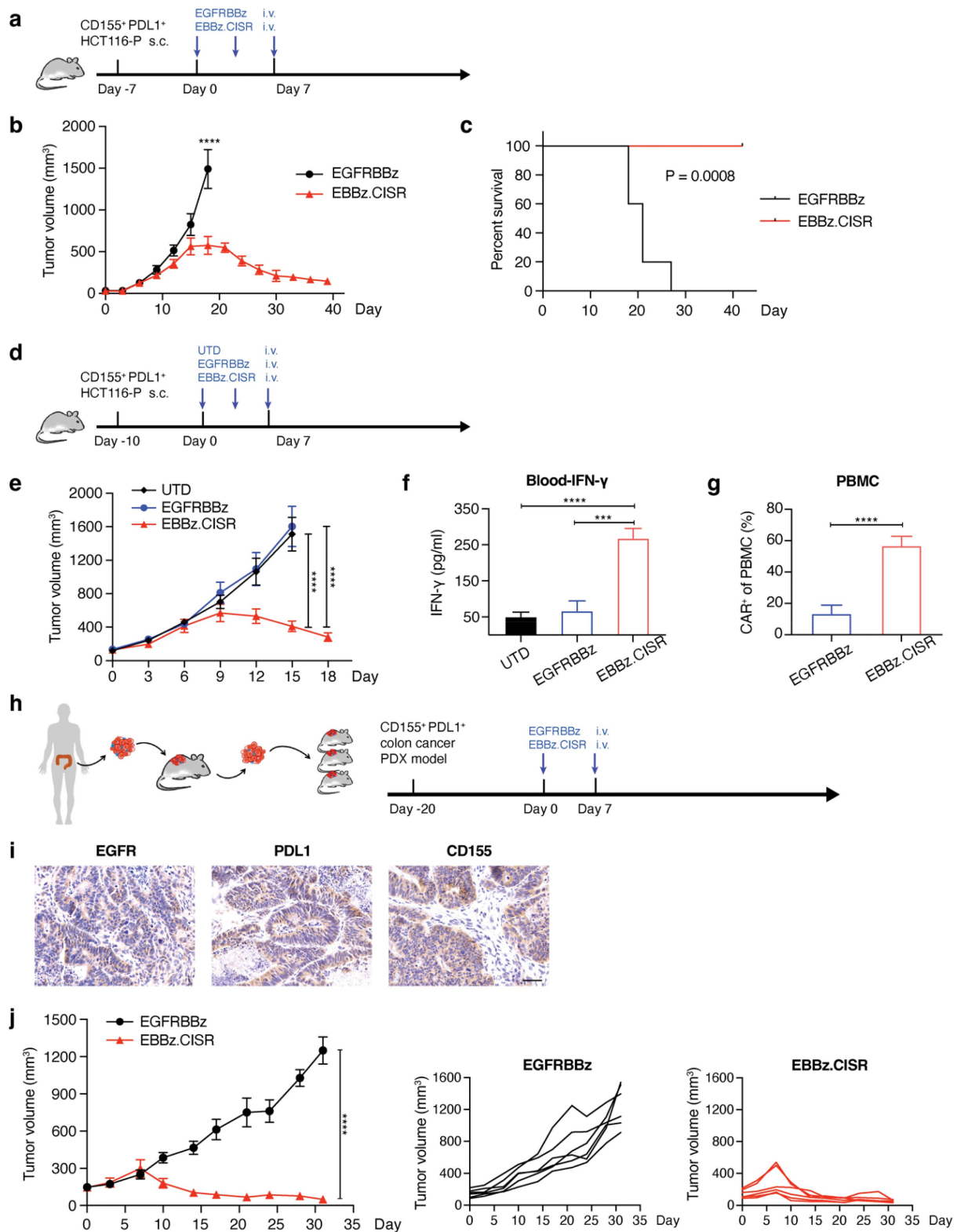
Figure 3. *In vivo* anti-tumor activity of EBBz.CISR in colorectal carcinoma cell-derived xenograft models and PDX models. (a-c) NPG mice bearing subcutaneous EGFR⁺PDL1⁺CD155⁺ HCT116-P cell-derived tumors were intravenously treated three times with 3×10^6 EGFRBBz-CAR T cells or EBBz.CISR T cells when tumor volumes reached 50–100 mm³. (a) schematic representation of the *in vivo* experiment. (b) tumor volume analysis at indicated time points (means ± SEMs, *n* = 5). Data were analyzed using two-way ANOVA; *P < .0001. (c) Kaplan-Meier survival curve. (d-g) NPG mice bearing subcutaneous HCT116-P cell-derived tumors were intravenously treated three times with 3×10^6 control T cells (untransduced, UTD) or CAR T cells when tumor volumes reached 100–200 mm³. (d) schematic representation of the *in vivo* experiment. (e) tumor volume analysis (means ± SEMs, *n* = 5). Data were analyzed using two-way ANOVA; **P < .0001. (f, g) Peripheral blood samples were collected from mice 2 weeks after treatment, and the levels of IFN-γ (f) and proportions of CAR-positive cells (g) were measured (means ± SEMs, *n* = 5). Statistical significance was analyzed using one-way ANOVA (f) and two-tailed Student's t-test (g); ***P < .001, ****P < .0001. (h-j) PDX tumor tissues were subcutaneously implanted into NPG mice. Approximately 20 days after implantation, when tumor volumes reached 100–200 mm³, mice received twice intravenous treatment with 3×10^6 EGFRBBz-CAR T cells or EBBz.CISR T cells. (h) schematic representation of PDX model development and CAR T cell treatment experiment. (i) expression patterns of EGFR, PDL1, and CD155 in tumor tissues used for PDX model establishment were analyzed by immunohistochemical staining. (j) analysis of mean tumor volume at indicated time points (left) (means ± SEMs, *n* = 6), along with tumor volume in each mouse (right). Data were analyzed using two-way ANOVA; *P < .0001.

poor prognosis.[26] Xenograft mouse models were used to evaluate the efficacy of EBBz.CISR T cells in the treatment of colorectal cancer. A dual suppressive tumor model was established with EGFR$^+$PDL1$^+$CD155$^+$ HCT116-P cells. When the tumor volume reached 50–100 mm^3, mice were treated with EGFRBBz-CAR or EBBz.CISR T cells (Figure 3a). Whereas EGFRBBz-CAR T cells did not control tumor growth, EBBz.CISR T cells significantly reduced tumor progression and volume (Figure 3b). Moreover, EBBz.CISR T cell treatment improved overall survival without causing significant weight loss (Figures 3c and S10). Similar results were observed with Ez.CISR T cells in this model (Figure S11a-c). We also performed a rechallenge experiment using the same tumor cells. All mice treated with EBBz.CISR T cells rejected rechallenged tumors, while the growth of rechallenged tumors could be observed in mice treated with EGFRBBz-CAR T cells after 2 weeks (Figure S12a-c).

The efficacy of EBBz.CISR T cells was explored in larger tumors (100–200 mm^3) (Figure 3d). Compared with controls, EBBz.CISR T cell treatment was more effective in reducing tumor size (Figure 3e). Greater IFN-γ release and a higher proportion of human CAR T cells were detected in the peripheral blood of mice treated with EBBz.CISR T cells (Figure 3f,g). Immunostaining revealed prominent human CD3$^+$ T cell infiltration in tumor tissues from EBBz.CISR T cell-treated mice; fewer T cells were observed in the control and EGFRBBz-CAR T cell groups (Figure S13a, b). Hematoxylin and eosin staining revealed increased necrosis within tumor tissues in the EBBz. CISR T cell group, such that few viable tumor cells remained (Figure S13c). Overall, EBBz.CISR T cells demonstrated improved persistence, infiltration, cytokine release, and enhanced anti-tumor activity *in vivo*, highlighting their potential in the treatment of colorectal carcinoma.

We also evaluated the effectiveness of EBBz.CISR T cells using PDX mouse models generated by transplanting colorectal cancer patient-derived tumor fragments expressing EGFR, PDL1, and CD155 into immunodeficient mice. When the tumor volume reached 100–200 mm^3, the mice were divided into two groups: EGFRBBz-CAR T cell and EBBz. CISR T cell (Figure 3h,i). Anti-tumor efficacy was assessed by monitoring changes in tumor volume. Tumors in the EGFRBBz-CAR T cell group displayed a continuous increase in volume; tumors in the EBBz.CISR T cell group gradually shrank, beginning 1 week after treatment (Figure 3j). At the end of the experiment, mice in the EBBz.CISR T cell group exhibited only small tumor tissues, whereas mice in the EGFRBBz-CAR T cell group displayed significantly larger tumors (Figure S14a). Hematoxylin and eosin staining confirmed that the remaining tissues in the EBBz.CISR T cell group primarily consisted of stromal cells, rather than tumor cells (Figure S14b). Furthermore, prominent human CD3$^+$ T cell infiltration was observed in EBBz.CISR T cell-treated tumors, surpassing the level of infiltration observed in the EGFRBBz-CAR T cell group (Figure S14c, d). Taken together, these results demonstrated that EBBz.CISR T cells were more effective in the treatment of colorectal cancer within an immunosuppressive environment, highlighting the potential for CISR use in cancer immunotherapy.

Discussion

Immune checkpoints, which play a key role in the suppression of engineered cellular immunotherapies, represent a major challenge. This study serves as a proof-of-concept for a CISR that simultaneously modulates two key immune checkpoints (PD1 and TIGIT). In T cells genetically modified to express the CISR, ligand binding of PD1, TIGIT, or both successfully triggered CD28 signaling, leading to enhanced T cell proliferation, cytokine release, cytotoxicity efficiency, and long-term anti-tumor activity. Through the reversal of inhibitory signaling and enhancement of anti-tumor activity in CAR T cells, the PD1-TIGIT CISR demonstrates considerable potential for cancer immunotherapy within an immunosuppressive tumor microenvironment.

Previous studies have utilized the combined co-stimulatory molecules CD28 and 4-1BB directly in third-generation CAR constructs to enhance immunotherapeutic efficacy.[27] In contrast, our CISR approach introduces an additional co-stimulatory signal specifically within the tumor microenvironment where PDL1 and CD155 are over-expressed. This design may restrict augmented T cell immune responses to the tumor site, minimizing off-tumor cytotoxicity and enhancing the safety profile of CISR-CAR T cells. And the CISR approach can be extended to combine with other low-affinity CARs or tumor specific TCRs to further enhance safety.[28] Moreover, the CISR has flexibility in terms of altering the ICD to various co-stimulation signals or positive cytokine signals, enabling further optimization of T cell activity.[29,30] The ECDs of the CISR could also be modified to target other immunosuppressive factors, including a variety of inhibitory receptor signals.[31] Consequently, diverse targeting designs can be developed to maximize the utility of the CISR strategy across malignancies. In summary, CISR has considerable potential as a strategy to improve immune cell function and overcome the challenges presented by immunosuppressive tumor microenvironments.

Author contributions

JZ, JD, and CD designed the research, performed the experiments, analyzed the data, and wrote the manuscript. SS wrote the manuscript. QZ and HL assisted with some experiments and provided technical assistance. YB and HD designed the research, supervised the research, and wrote the manuscript.

Data availability statement

The authors confirm that the data supporting the findings of this study are available within the article and its supplementary materials.

References

1. June CH, Sadelain M. Chimeric antigen receptor therapy. N Engl J Med. 2018;379(1):64–73. doi:10.1056/NEJMra1706169.
2. June CH, O'Connor RS, Kawalekar OU, Ghassemi S, Milone MC. CAR T cell immunotherapy for human cancer. Science. 2018;359 (6382):1361–1365. doi:10.1126/science.aar6711.
3. Pardoll DM. The blockade of immune checkpoints in cancer immunotherapy. Nat Rev Cancer. 2012;12(4):252–264. doi:10.1038/nrc3239.
4. Anderson AC, Joller N, Kuchroo VK. Lag-3, tim-3, and TIGIT: co-inhibitory receptors with specialized functions in immune regulation. Immunity. 2016;44(5):989–1004. doi:10.1016/j.immuni.2016.05.001.
5. Zou W, Chen L. Inhibitory B7-family molecules in the tumour microenvironment. Nat Rev Immunol. 2008;8(6):467–477. doi:10.1038/nri2326.
6. Johnston RJ, Comps-Agrar L, Hackney J, Yu X, Huseni M, Yang Y, Park S, Javinal V, Chiu H, Irving B, et al. The immunoreceptor TIGIT regulates antitumor and antiviral CD8(+) T cell effector function. Cancer Cell. 2014;26(6):923–937. doi:10.1016/j.ccell.2014.10.018.
7. Chauvin JM, Pagliano O, Fourcade J, Sun Z, Wang H, Sander C, Kirkwood JM, Chen TH, Maurer M, Korman AJ, et al. TIGIT and PD-1 impair tumor antigen-specific CD8(+) T cells in melanoma patients. J Clin Invest. 2015;125(5):2046–2058. doi:10.1172/JCI80445.
8. Liu X, Li M, Wang X, Dang Z, Jiang Y, Wang X, Kong Y, Yang Z. PD-1(+) TIGIT(+) CD8(+) T cells are associated with pathogenesis and progression of patients with hepatitis B virus-related hepatocellular carcinoma. Cancer Immunol Immunother. 2019;68 (12):2041–2054. doi:10.1007/s00262-019-02426-5.
9. Grosser R, Cherkassky L, Chintala N, Adusumilli PS. Combination immunotherapy with CAR T cells and checkpoint blockade for the treatment of solid tumors. Cancer Cell. 2019;36(5):471–482. doi:10.1016/j.ccell.2019.09.006.
10. Liu X, Ranganathan R, Jiang S, Fang C, Sun J, Kim S, Newick K, Lo A, June CH, Zhao Y, et al. A chimeric switch-receptor targeting PD1 augments the efficacy of second-generation CAR T cells in advanced solid tumors. Cancer Res. 2016;76(6):1578–1590. doi:10.1158/0008-5472.CAN-15-2524.
11. Hoogi S, Eisenberg V, Mayer S, Shamul A, Barliya T, Cohen CJ. A TIGIT-based chimeric co-stimulatory switch receptor improves T-cell anti-tumor function. J Immunother Cancer. 2019;7(1):243. doi:10.1186/s40425-019-0721-y.
12. Chen C, Gu YM, Zhang F, Zhang ZC, Zhang YT, He YD, Wang L, Zhou N, Tang FT, Liu HJ, et al. Construction of PD1/CD28 chimeric-switch receptor enhances anti-tumor ability of c-met CAR-T in gastric cancer. Oncoimmunology. 2021;10(1):1901434. doi:10.1080/2162402X.2021.1901434.
13. Banta KL, Xu X, Chitre AS, Au-Yeung A, Takahashi C, O'Gorman WE, Wu TD, Mittman S, Cubas R, Comps-Agrar L, et al. Mechanistic convergence of the TIGIT and PD-1 inhibitory pathways necessitates co-blockade to optimize anti-tumor CD8+ T cell responses. Immunity. 2022;55(3):512–526.e9. doi:10.1016/j.immuni.2022.02.005.
14. Lee YH, Lee HJ, Kim HC, Lee Y, Nam SK, Hupperetz C, Ma JSY, Wang X, Singer O, Kim WS, et al. PD-1 and TIGIT downregulation distinctly affect the effector and early memory phenotypes of CD19-targeting CAR T cells. Mol Ther. 2022;30(2):579–592. doi:10.1016/j.ymthe.2021.10.004.
15. Hung AL, Maxwell R, Theodros D, Belcaid Z, Mathios D, Luksik AS, Kim E, Wu A, Xia Y, Garzon-Muvdi T, et al. TIGIT and PD-1 dual checkpoint blockade enhances antitumor immunity and survival in GBM. Oncoimmunology. 2018;7(8):e1466769. doi:10.1080/2162402X.2018.1466769.
16. Deng C, Zhao J, Zhou S, Dong J, Cao J, Gao J, Bai Y, Deng H. The vascular disrupting agent CA4P improves the antitumor efficacy of CAR-T cells in preclinical models of solid human tumors. Mol Ther. 2020;28(1):75–88. doi:10.1016/j.ymthe.2019.10.010.
17. Sun Q, Zhou S, Zhao J, Deng C, Teng R, Zhao Y, Chen J, Dong J, Yin M, Bai Y, et al. Engineered T lymphocytes eliminate lung metastases in models of pancreatic cancer. Oncotarget. 2018;9 (17):13694–13705. doi:10.18632/oncotarget.24122.
18. Sun C, Mezzadra R, Schumacher TN. Regulation and function of the PD-L1 checkpoint. Immunity. 2018;48(3):434–452. doi:10.1016/j.immuni.2018.03.014.
19. Gao J, Zheng Q, Xin N, Wang W, Zhao C. CD155, an onco-immunologic molecule in human tumors. Cancer Sci. 2017;108(10):1934–1938. doi:10.1111/cas.13324.
20. Keir ME, Sharpe AH. The B7/CD28 costimulatory family in autoimmunity. Immunol Rev. 2005;204(1):128–143. doi:10.1111/j.0105-2896.2005.00242.x.
21. Esensten JH, Helou YA, Chopra G, Weiss A, Bluestone JA. CD28 costimulation: from mechanism to therapy. Immunity. 2016;44 (5):973–988. doi:10.1016/j.immuni.2016.04.020.
22. Katsarou A, Sjostrand M, Naik J, Mansilla-Soto J, Kefala D, Kladis G, Nianias A, Ruiter R, Poels R, Sarkar I, et al. Combining a CAR and a chimeric costimulatory receptor enhances T cell sensitivity to low antigen density and promotes persistence. Sci Transl Med. 2021;13(623):eabh1962. doi:10.1126/scitranslmed.abh1962.
23. Riley JL. PD-1 signaling in primary T cells. Immunol Rev. 2009;229 (1):114–125. doi:10.1111/j.1600-065X.2009.00767.x.
24. Liu Q, Sun Z, Chen L. Memory T cells: strategies for optimizing tumor immunotherapy. Protein Cell. 2020;11(8):549–564. doi:10.1007/s13238-020-00707-9.
25. Sung H, Ferlay J, Siegel RL, Laversanne M, Soerjomataram I, Jemal A, Bray F. Global cancer statistics 2020: GLOBOCAN estimates of incidence and mortality worldwide for 36 cancers in 185 countries. CA Cancer J Clin. 2021;71(3):209–249. doi:10.3322/caac.21660.
26. Zhou X, Ding X, Li H, Yang C, Ma Z, Xu G, Yang S, Zhang D, Xie X, Xin L, et al. Upregulation of TIGIT and PD-1 in colorectal cancer with mismatch-repair deficiency. Immunol Invest. 2020;50 (4):1–18. doi:10.1080/08820139.2020.1758130.
27. Carpenito C, Milone MC, Hassan R, Simonet JC, Lakhal M, Suhoski MM, Varela-Rohena A, Haines KM, Heitjan DF, Albelda SM, et al. Control of large, established tumor xenografts with genetically retargeted human T cells containing CD28 and CD137 domains. Proc Natl Acad Sci U S A. 2009;106 (9):3360–3365. doi:10.1073/pnas.0813101106.
28. Drent E, Themeli M, Poels R, de Jong-Korlaar R, Yuan H, de Bruijn J, Martens ACM, Zweegman S, van de Donk N, Groen RWJ, et al. A rational strategy for reducing on-target off-tumor effects of CD38-chimeric antigen receptors by affinity optimization. Mol Ther. 2017;25(8):1946–1958. doi:10.1016/j.ymthe.2017.04.024.
29. Wang Y, Jiang H, Luo H, Sun Y, Shi B, Sun R, Li Z. An IL-4/21 inverted cytokine receptor Improving CAR-T cell potency in immunosuppressive solid-tumor microenvironment. Front Immunol. 2019;10:1691. doi:10.3389/fimmu.2019.01691.
30. Ma X, Shou P, Smith C, Chen Y, Du H, Sun C, Porterfield Kren N, Michaud D, Ahn S, Vincent B, et al. Interleukin-23 engineering improves CAR T cell function in solid tumors. Nat Biotechnol. 2020;38(4):448–459. doi:10.1038/s41587-019-0398-2.
31. Lin S, Cheng L, Ye W, Li S, Zheng D, Qin L, Wu Q, Long Y, Lin S, Wang S, et al. Chimeric CTLA4-CD28-CD3z T cells potentiate antitumor activity against CD80/CD86-positive B cell malignancies. Front Immunol. 2021;12:642528. doi:10.3389/fimmu.2021.642528.